High-Reliability Photovoltaic Converter Based on Improved PSO Algorithm

Yang Jingfan, *Ge Hongjuan**, *Yang Fan*

College of Automation, Nanjing University of Aeronautics and Astronautics, Nanjing 210016, P. R. China

(Received 8 March 2018; revised 2 May 2018; accepted 10 May 2018)

Abstract: An improved particle swarm optimization(PSO) algorithm based on dynamic inertia weight and adjustment coefficient is proposed in this paper. The expressions of inertia weight and adjustment coefficient are established based on inter-particle distance and iterations. The improved algorithm is applied to a novel two-stage photovoltaic(PV) converter. The later DC/AC circuit chooses a dual-DC-input multi-level dual-buck inverter. This converter has the advantages of no shoot-through problem and high efficiency. Finally, the validity and effectiveness of the algorithm and the converter are verified with experimental results.

Key words: high reliability; photovoltaic converter; PSO algorithm

CLC number: TM464 **Document code**: A **Article ID**: 1005-1120(2018)S-0068-07

0 Introduction

The power produced by a PV module depends on the solar irradiance and temperature. When the PV array is shadowed by clouds, trees or buildings, the output curves will have multi peaks. Therefore, the conventional Maximum Power Point Tracking(MPPT) algorithms are not able to extract true maximum power. PSO algorithm has a great advantage in nonlinear curve optimization[1-2]. But applying PSO algorithm directly will cause large oscillation and slow tracking speed of the system. Some research groups have been made attempts in the global MPPT realization by evolving the PSO algorithm. Refs. [3-4] proposed a MPPT algorithm by introducing PSO technique. The proposed algorithm used only one controller with one pair of current and voltage sensors to control multiple PV arrays. Ref. [5] proposes the parameter turning method of the PSO controller based on an adjusting rule. But it is difficult to examine which value is the most effective by evaluating the tracking function to the power generation efficiency, optimum voltage and electric power in each control parameters.

Besides the MPPT algorithm, DC-AC inverters are the significant interfaces between solar array and AC load or grid. Among various inverter topologies, the dual buck inverter is promising because it has many advantages such as high reliability, no dead-time requirement and low common-mode leakage current[6]. However, the voltages of renewable sources are usually low. A front-end Boost converter is required to boot the low voltage to a high voltage level[7-8].

An improved PSO algorithm based on dynamic inertia weight and adjustment coefficient is proposed in this paper, which is used under partial shading conditions. The relationships between inertia weight, adjustment coefficient and inter-particle distance, iterations are built in accordance with fitness value of each particle. Meanwhile, a novel high-reliability PV converter is studied in this paper, which will be used to realize the PSO algorithm. Finally, the feasibility and efficiency of this system is verified by simulation and experiment.

* Corresponding author, E-mail address: allenge@nuaa.edu.cn.

How to cite this article: Yang Jingfan, Ge Hongjuan, Yang Fan. High-reliability photovoltaic converter based on improved PSO algorithm[J]. Trans. Nanjing Univ. Aeronaut. Astronaut., 2018,35(S):68-74.
http://dx.doi.org/10.16356/j.1005-1120.2018.S.068

1 Improved PSO Algorithm

Particle swarm optimization(PSO) algorithm is a specific embodiment of the swarm intelligence, which is presented by Kennedy and Eberhart in 1995[9]. The PSO is applied to the photovoltaic MPPT, and the output voltage of the solar array can be regarded as the flying particles flying to the MPP. The flight distance and direction of the particles are determined by the flight speed, which is determined by the individual optimal value and the global optimal value[10]. The flight velocity and position updating formula of each particle are as follows

$$\begin{cases} v_i^{k+1} = \omega v_i^k + c_1 r_1 (p_{\text{ibest}} - x_i^k) + c_2 r_2 (g_{\text{best}} - x_i^k) \\ x_i^{k+1} = v_i^{k+1} + x_i^k \end{cases} \tag{1}$$

The updating procedure of individual optimal value is as follows

$$p_i^{k+1} = \begin{cases} p_i^k & f(x_i^{k+1}) \leqslant f(p_i^k) \\ x_i^{k+1} & f(x_i^{k+1}) \geqslant f(p_i^k) \end{cases} \tag{2}$$

The updating procedure of global optimal value is as follows

$$p_g^{k+1} = \begin{cases} p_g^k & f(x_i^{k+1}) \leqslant f(p_g^k) \\ x_i^{k+1} & f(x_i^{k+1}) \geqslant f(p_g^k) \end{cases} \tag{3}$$

where ω is inertia weight, keeping the inertia motion; c_1 and c_2 adjustment coefficients between 0—2; r_1 and r_2 independent random numbers between 0—1; p_i^k the individual optimal value in the k-th cycle; p_g^k the global optimal value in the k-th cycle.

Obviously, inertia weight ωdetermines the effect of the previous iteration speed on the current iteration[11-12]. In the early stages, the weight value should be set larger so that the algorithm is not easy to jump into local optimization. In the late search period, ω should be smaller to improve the local search ability of the algorithm. At the initialization time, the particles which are distributed around the GMPP may jump out of the global optimum range because of the large inertia weight. Therefore, the inter-particle distance is used in this paper to adjust each particle's inertia weight value. The expression is as follows

$$\omega = \omega_{\max} - \frac{(\omega_{\max} - \omega_{\min}) \cdot (L_{ig} - L_{\min}) \cdot k}{k_{\max} \cdot (L_{\max} - L_{\min})} \tag{4}$$

L_{ig} is the distance of particle$i$ from the global optimum particle in the k-th cycle.

The adjustment coefficient can affect the velocity of the particle moving at the optimal position and the position of the global optimum. In the early stage, c_1 should be larger and c_2 should be smaller to avoid falling into the local MPP. In the late search, the situation should be opposite to make the system converge fast. Therefore, the expressions are established as follows

$$\begin{cases} c_1 = (c_{1\max} - c_{1\min}) \times \dfrac{k_{\max} - k}{k_{\max}} + c_{1\min} \\ c_2 = (c_{2\min} - c_{2\max}) \times \dfrac{k_{\max} - k}{k_{\max}} + c_{2\max} \end{cases} \tag{5}$$

According to the convergence analysis Refs. [13-15], when the relations between the parameters satisfy the next formula, particles will converge to the extreme point.

$$\omega > \frac{1}{2}(c_1 + c_2) - 1, \omega < 1, c_1 + c_2 > 0 \tag{6}$$

The values of each parameter will be given in the simulation and experiment part.

2 High-Reliability Photovoltaic Conversion System

2.1 Dual-input dual-buck inverter

As shown in Fig. 1, the topology can be named DB5 inverter because five active switches are used. V_{H} and V_{L} are the high voltage and low voltage DC port respectively. In comparison with the traditional dual-buck inverters, the extended low voltage DC-input port, whose voltage is lower than the peak amplitude of the AC output voltage, is able to supply power to the AC output within single-stage power conversion stage. Obviously, each bridge arm has a diode so that the topology has no shoot-through problem. Thus the reliability can be improved. Equivalent circuits of each switching state are given in Fig. 2.

It is easy to see from the switching states that S_1, S_2 and S_3 are high frequency switches, while S_4 and S_5 are low frequency switches. When the AC output voltage is lower than the

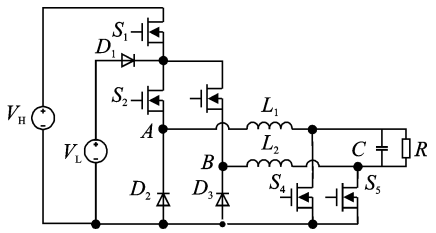

Fig. 1 Topologies of dual-input DB5 inverter

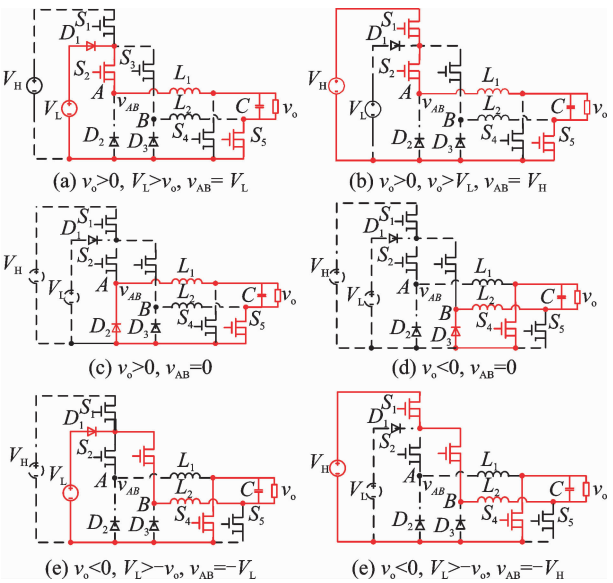

Fig. 2 Equivalent circuit of each switching state

low voltage port V_L, the low voltage port supplies power to AC output only. While the AC output voltage is larger, the high voltage port begins to supply power. Dual carrier modulation technique is used and its waveforms are shown in Fig. 3.

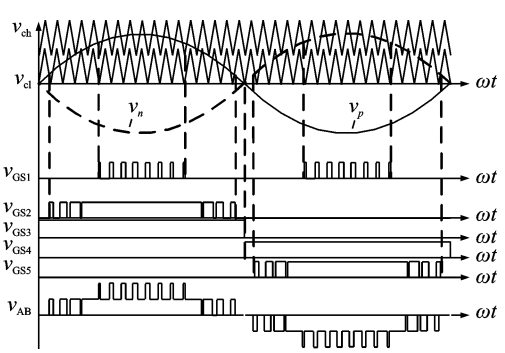

Fig. 3 Dual carrier modulation waveforms

Two carrier signals v_{cl} and v_{ch} are used and compared with the control signals v_p and v_n, the modulated sine wave in positive and negative cycle respectively. The DB5 inverter has six switching states and the high frequency voltage generated between the mid-points of the two switching bridges v_{AB} has five voltage levels. The multi-level characteristic can help to reduce the switching losses and size of the output filter effectively.

2.2 Two-Stage photovoltaic converter

Boost circuit, a single-tube non-isolated DC converter, is usually used in PV system to realize MPPT algorithm because of its simple topology and the ability to work in the state of continuous current. The Boost circuit can increase the low output voltage of the PV array to meet the needs of the post-stage inverter (Fig. 4).

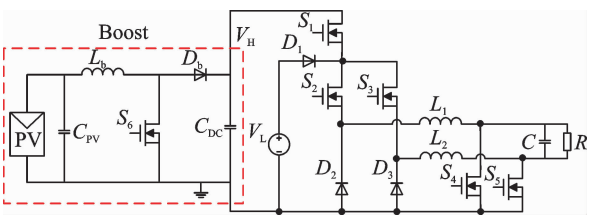

Fig. 4 Two-stage photovoltaic converter

Usually, the duty cycle of the switch in Boost circuit is used as the control variable in MPPT methods. The characteristics of PV array show that the equivalent impedance determines the operating point of the PV array. In this system, the DC bus voltage VH must be controlled within a reasonable scope in order to ensure the normal operation of the inverter. The control strategy is shown in Fig. 5.

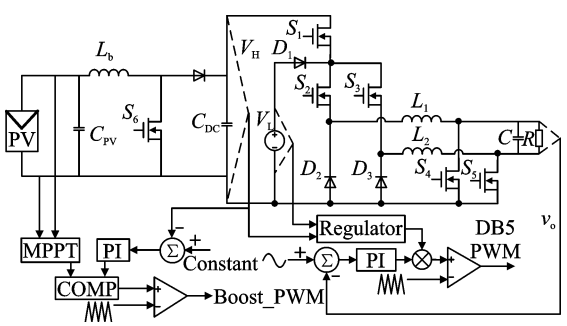

Fig. 5 Control chart of the two-stage photovoltaic converter

The AC output voltage of the inverter is 220 V/50 Hz and the peak value vom is 311 V so that the DC bus voltage VH should be higher than 311 V. Meanwhile, the voltage stress of devices cause the DC bus voltage to be limited in

a safe range. PSO algorithm is used in the safe range but if it is out of the range, PI regulator will work to control the voltage. The values of voltage V_H and V_L are not fixed and this cause the amplitude of the PWM modulation wave v_{ea} of the inverter to be adjusted timely. The relationship of v_{ea} and the amplitude of the carrier v_c is as follows

$$\frac{v_{ea}}{v_c}=\frac{v_{om}}{V_H} \tag{7}$$

v_c is the sum of the amplitude of the two carriers v_{cl} and v_{ch}, and they have the relationship as

$$\frac{v_{cl}}{v_{ch}}=\frac{V_L}{V_H-V_L} \tag{8}$$

However in application, the amplitude of the carrier is fixed because of the fixed frequency of switches. Thus the amplitude of v_{ea} which is the output of the PI regulator should be adjusted according to the DC inputs.

3 Simulation and Experimental Verification

3.1 Simulation verification

Firstly, the feasibility of the improved PSO algorithm is verified. The parameters of HBM (175) solar cell are adopted in simulation: Open-circuit voltage $U_{oc}=44.2$ V, voltage at the maximum power point $U_m=35.4$ V, short-circuit current $I_{oc}=5.29$ A, current at the maximum power point $I_m=4.95$ A. The reference temperature is 25°C and the reference illumination is 1 000 W/m^2. The PV characteristic curves under different partial conditions are shown in Fig. 6, which will be used to verify the feasibility of the improved PSO algorithm.

The simulation is realized in the MATLAB. The simulation time is 0.01s and step size is $1e^{-7}$ s. The parameters of the improved PSO algorithm are given: The range of inertia weight is [0.4,1], the range of adjustment coefficients is [1,2]. The maximum number of iteration k_{max} is related to the search scope and step length and the value is 30 in this simulation. The simulation results are shown in Fig. 7 and the feasibility of the improved PSO algorithm can be verified.

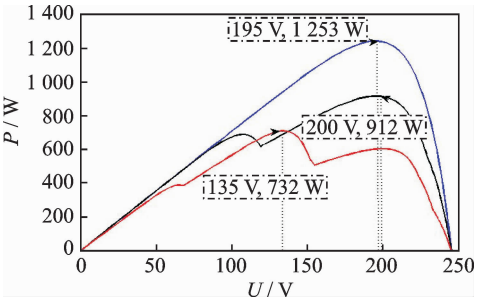

Fig. 6 PV curves under different partial shade conditions

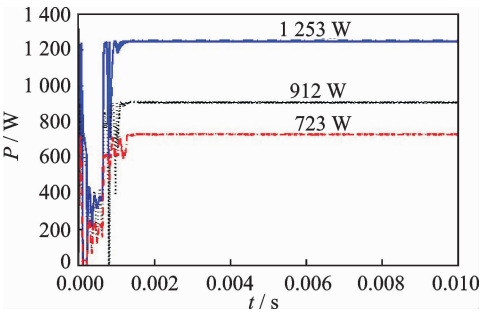

Fig. 7 Simulation results of PSO algorithm

The simulation model of the two-stage photovoltaic converter is established, where the inductance value of boost circuit $L_b=1.5$ mH, the DC bus capacitor $C_{DC}=1$ mF, the output filter inductance value of inverter $L_1=L_2=3$ mH, the output filter capacitor $C=1$ μF and the resistance $R=48.4$ Ω. The simulation results of the front-end boost circuit are shown in Fig. 8. The power of PV modules PPV can reach the maximum and the DC bus voltage V_H is getting larger to meet the needs of the later inverter. Inductor current I_{LB} has little pulsation in steady state.

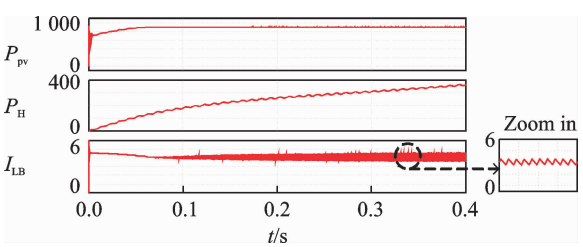

Fig. 8 Simulation results of the front-end boost circuit

The high-voltage port and low-voltage port input currents of inverter I_H and I_L, as well as the currents of the output filter inductors I_{L1} and I_{L2} are as Fig. 9.

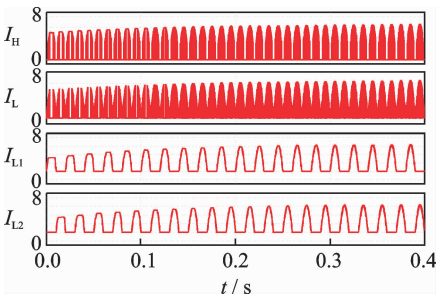

Fig. 9 Simulation waveforms of I_H, I_L, I_{L1} and I_{L2}

The voltage between the mid-points of the two switching legs v_{AB} and the output voltage v_o are shown in Fig. 10. The two inductors works only in half-period of the output voltage. It can be seen that three voltage levels are generated by each switching leg and five voltage levels are obtained from the mid-points of the two switching legs.

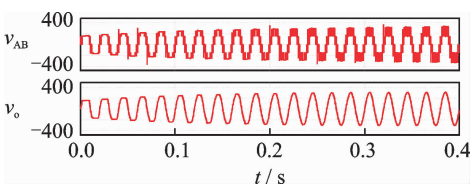

Fig. 10 Simulation waveforms of v_{AB} and v_o

3.2 Experimental results

A 1kW prototype is built and tested to verify the effectiveness of the proposed two-stage photovoltaic converter and the improved PSO algorithm. The voltage VL of the low voltage source is 150—300 V, and the AC output voltage vo is 220 V/50 Hz. A Boost converter is employed as the front-end DC/DC converter to realize the MPPT algorithm. The switching frequency of the Boost circuit is 50 kHz and the switching frequency of the inverter is 20 kHz. The devices used are as follows. S1: IXFH69N30P, S2 and S3: SPW52N50C3, S4 and S5: IPW65R048CFDA, S6: SPW47N60CFD, D1: DPG30C300HB, D2 and D3: DSEC30-06A, Db: HFA30PA60C. The values of inductors and capacitors are as same as simulation.

The PV output characteristics are simulated using Chroma company's 62050 photovoltaic simulator and the parameters are set as Table 1.

Table 1 Parameters of Photovoltaic Simulator

Symbol	Quantity	Value
V_{OC}	open-circuit voltage	251.5V
I_{SC}	short-circuit current	5.858A
V_{MP}	voltage at the MPP	197.2V
I_{MP}	current at the MPP	5.174A
P_{MP}	power at the MPP	1020W

The output voltage of the photovoltaic simulator is shown in Fig. 11. It can be seen that the maximum power point can be tracked using this algorithm.

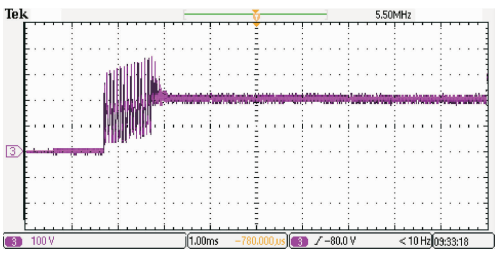

Fig. 11 Experimental waveform of PV output voltage

When the system works steadily, waveforms of Boost circuit and inverter are as shown in Figs. 12, 13, respectively. The DC bus voltage V_H is 394V, which is connected to the high voltage port of late DC/AC inverter. V_{gS6} and V_{ds} are the gate-source voltage and drain-source voltage of switch S_6.

It can be seen from Fig. 13(a) that the switch S_5 is always on in the positive half-cycle of vo. When V_L is lower than the peak amplitude of the

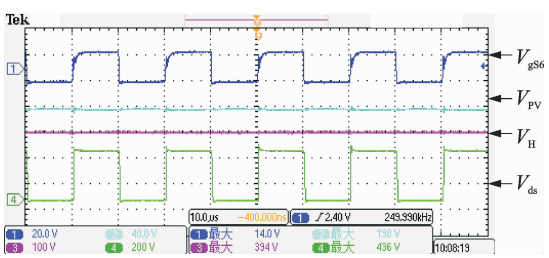

Fig. 12 Experimental waveforms of V_{gS6}, V_{PV}, V_H and V_{ds}

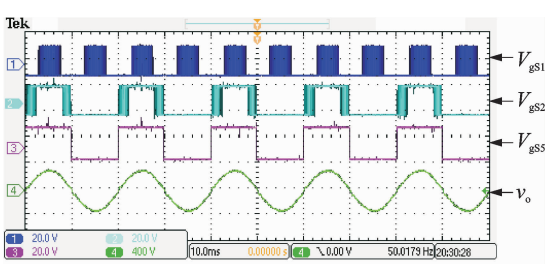

(a) Experimental waveforms of driving and output voltages

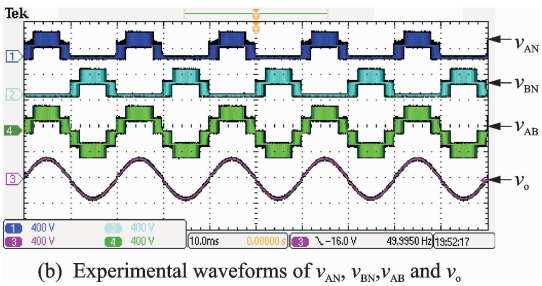

(b) Experimental waveforms of v_{AN}, v_{BN}, v_{AB} and v_o

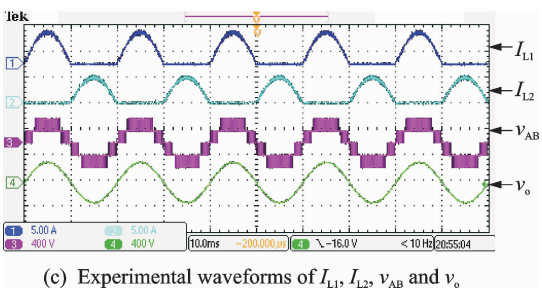

(c) Experimental waveforms of I_{L1}, I_{L2}, v_{AB} and v_o

Fig. 13 Experimental results of dual-input DB5 inverter

AC output voltage, the two switches S_1 and S_2 work in high frequency alternatively. When $V_L > v_o$, S_2 operates in high frequency while S_1 is kept in OFF state. When $V_L < v_o$, S_2 keeps on and S_1 works in high frequency. The output voltages v_{AN} and v_{BN} of two high frequency switching legs, the voltage between the mid-points of the two switching legs v_{AB} and the output voltage are shown in Fig. 13(b). It can be seen that three voltage levels are generated by each switching leg, and five voltage levels are obtained from the mid-points of the two switching legs. The currents of the two filter inductors I_{L1} and I_{L2}, the mid-point voltage v_{AB} and the output voltage v_o are shown in Fig. 13(c).

4 Conclusion

In this paper, a novel dual-input dual-buck inverter is presented and used in photovoltaic conversion system. A low voltage DC source is connected to the inverter and supplies power to the AC load directly. An improved PSO algorithm is adopted to realize maximum power point tracking. The simulation and experimental results verify the correctness and rationality of the proposed algorithm. Meanwhile, the feasibility and reliability of the photovoltaic converter are also verified. This provides a new choice for aviation electrical applications in the future.

References:

[1] XU G, HU G C. Application of new PSO hybrid algorithm to helicopter trim[J]. Journal of Nanjing University of Aeronautics & Astronautics, 2016, 48(3):426-431. (in Chinese)

[2] LIN S, WANG G L. Warehouse environment parameter monitoring system and sensor error correction model based on PSO-BP[J]. Transactions of Nanjing University of Aeronautics & Astronautics, 2017, 34(3):333-340.

[3] MASAFUMI M, VEERACHARY M, TORIUMI F, et al. Maximum power point tracking of multiple photovoltaic arrays: A PSO approach[J]. IEEE Transactions on Aerospace &ElectronicSystems, 2011, 47(1):367-380.

[4] KENNEDY J, BERHART R. Particle swarm optimization[C]// IEEE International Conference on Neural Networks. Nagoya Japan: IEEE, 1995: 1942-1948.

[5] KAMEJIMA T, PHIMMASONE V, KONDO Y, et al. The optimization of control parameters of PSO based MPPT for photovoltaics[C]// IEEE Ninth International Conference on Power Electronics and Drive Systems. Singapore: IEEE, 2011: 881-883.

[6] YANG F, GE H J, YANG J F, et al. An asymmetrical multi-level dual-input dual-buck inverter for multi-source interface applications[C]// IEEE Applied Power Electronics Conference and Exposition. Tampa F L USA: IEEE, 2017: 2228-2233.

[7] DING G, GAO F, TIAN H, et al. Adaptive DC-link voltage control of two-stage photovoltaic inverter during low voltage ride-through operation[J]. IEEE Transactions on Power Electronics, 2016, 31(6): 4182-4194.

[8] HU Cungang, YAO Pei, ZHANG Yunlei, et al. Topology and control strategy for high-efficient non-isolated single-phase grid- connected MOSFET inverter [J]. Transactions of China Electrotechnical Society, 2016, 31(13): 82-91.

[9] HAN H X. Research on MPPT algorithm of PV array under local shadow[D]. Hangzhou: Zhejiang University, 2014.

[10] ZHENG Y B, WANG W, CHEN W, et al. Research on MPPT of photovoltaic system based on PSO under partial shading condition[C]// Chinese Control Conference TCCT. Chengdu, China: [s. n.], 2016: 8654-8659.

[11] ISHAQUE K, SALAM Z, TAHERI H, et al. Maximum power point tracking for PV system under partial shading condition via particle swarm optimization [C]// Applied Power Electronics Colloquium. IEEE, 2011:5-9.

[12] ISHAQUE K, SALAM Z, TAHERI H. Simple, fast and accurate two-diode model for photovoltaic modules[J]. Solar Energy Materials & Solar Cells, 2011, 95(2):586-594.

[13] ZHANG L. Theory and practice of particle swarm optimization [D]. Hangzhou: Zhejiang University, 2005.

[14] LIU B N, ZHANG W G. Improved multi-object particle swarm optimization algorithm [J]. Journal of Beijing University of Aeronautics and Astronautics, 2013,(4):458-462,473.

[15] SHI J Y, ZHANG W, ZHANG Y G, et al. Research of photovoltaic array MPPT based on improved PSO algorithm[J]. Electric Drive, 2015, 45(7): 52-55.

Ms. **Yang Jingfan** received the B. S. degree in electrical engineering from Nanjing University of Aeronautics and Astronautics(NUAA), Nanjing, China, in 2015. She is currently working for the M. S. degree in electrical engineering from NUAA, Nanjing, China. Her research interests include topology and control of DC-AC converters.

Prof. **Ge Hongjuan** received the B. S. and M. S degrees in Engineering from Southeast University, Nanjing, China, in 1985 and 1988, respectively, and the Ph. D. degree in Electrical Engineering from Nanjing University of Aeronautics and Astronautics, Nanjing, China, in 2007. She joined the Faculty of Electrical Engineering, NUAA in 1988 and is currently a Professor at the Electrical Engineering Department, College of Automation Engineering. Her research interests include topology and control for AC-AC-Matrix Converters, and PMSM drive and Control. She has authored more than 30 technical papers published in journals and conference proceedings.

Ms. **Yang Fan** received the B. S. degree in electrical engineering from Nanjing Normal University, Nanjing, China, in 2007, and the M. S degree in electrical engineering from Nanjing University of Aeronautics and Astronautics, Nanjing, China, in 2013. She is currently working toward the Ph. D. degree in electrical engineering and power drives from NUAA, Nanjing, China. Her research interests include topology and control of DC-DC and DC-AC converters.

(Production Editor: Liu Yandong)